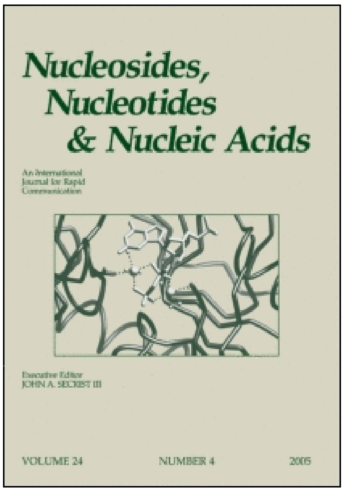

Nucleosides, Nucleotides and Nucleic Acids
Publication details, including instructions for authors and subscription information:
http://www.informaworld.com/smpp/title~content=t713597286

MOLECULAR MODELLING OF 2'-OH MEDIATED HYDROGEN BONDING IN RIBONUCLEOS(T)IDES BY NMR CONSTRAINED AM1 AND MMX CALCULATIONS

Parag Acharya[a]; Irina Velikian[a]; Sandipta Acharya[a]; Jyoti Chattopadhyaya[a]
[a] Department of Bioorganic Chemistry, Box 581, Biomedical Centre, University of Uppsala, Uppsala, Sweden

To cite this Article Acharya, Parag , Velikian, Irina , Acharya, Sandipta and Chattopadhyaya, Jyoti(2001) 'MOLECULAR MODELLING OF 2'-OH MEDIATED HYDROGEN BONDING IN RIBONUCLEOS(T)IDES BY NMR CONSTRAINED AM1 AND MMX CALCULATIONS', Nucleosides, Nucleotides and Nucleic Acids, 20: 4, 1211 — 1217

To link to this Article: DOI: 10.1081/NCN-100002521

URL: http://dx.doi.org/10.1081/NCN-100002521

NUCLEOSIDES, NUCLEOTIDES & NUCLEIC ACIDS, 20(4–7), 1211–1217 (2001)

MOLECULAR MODELLING OF 2′-OH MEDIATED HYDROGEN BONDING IN RIBONUCLEOS(T)IDES BY NMR CONSTRAINED AM1 AND MMX CALCULATIONS

Parag Acharya, Irina Velikian, Sandipta Acharya,
and Jyoti Chattopadhyaya*

Department of Bioorganic Chemistry, Box 581, Biomedical Centre,
University of Uppsala, S-751 23 Uppsala, Sweden

ABSTRACT

The intra- and intermolecular hydrogen bonding ($\Delta G^{\circ}_{298K} \approx 2$ kcal mol^{-1}) of 2′-OH in nucleos(t)ides has been reported by the temperature- and concentration-dependent NMR study in conjunction with dihedral dependence of the NMR derived both endo ($^{3}J_{H,H}$)- and exocyclic ($^{3}J_{H,OH}$) coupling constants, nOe contacts and lineshape analyses of hydroxyl protons for EtpA (**1**), 3′-dA (**2**), rA (**3**), 2′-dA (**4**) [Fig. 1] in DMSO-d_6 at 500 MHz.

The 2′-hydroxyl group has a major structural implications in RNA recognition, processing and catalytic properties (1a). Clearly, the nature of involvement of the 2′-OH group in the intra- and intermolecular hydrogen bonding (1b) in nucleos(t)ides will determine its chemical reactivity in the biological systems. The downfield shift of the hydroxyl protons [δ_{OH}] for **1**–**4** with lowering of temperature (Table 1) has been correlated with the strength of the H-bonding (2a). In **1**, the electron withdrawing effect of the vicinal 3′-ethylphosphate as well as intramolecular 2′-O-H$\cdots$O3′ H-bonding (as evident by 16 line multiplicity of the non-equivalent methylene protons, *vide infra*) makes its $\delta_{2'OHeq}$ to resonate most downfield (7.305 ppm) compared to $\delta_{2'OHax}$ in **2** (5.584 ppm) and $\delta_{2'OHeq}$ in **3** (5.365 ppm) at 298 K. According to

---

*Corresponding author. Fax: (+46) 185-54-495; E-mail: Jyoti.Chattopadhyaya@BioorgChem.uu.se

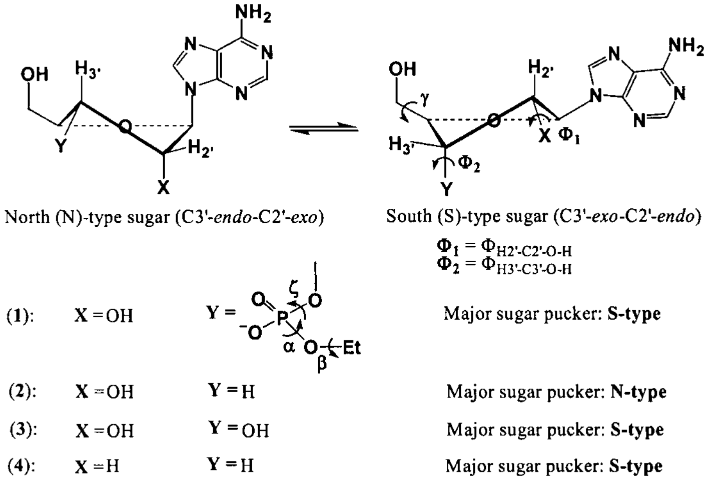

Figure 1. The schematic representation of the bias of the dymanic two-state pseudorotational equilibrium between the North-type (N, C2′-*exo* -C3′-*endo*) and the South-type (S, C3′-*exo*-C2′-*endo*) (3a) pseudorotamers of the sugar moeity for EtpA (**1**), 3′-dA (**2**), rA (**3**), 2′-dA (**4**) and torsion (Φ) around C2′/3′-O bond *viz.* $\Phi_1 = \Phi_{H2'\text{-}C2'\text{-}O\text{-}H}$ and $\Phi_2 = \Phi_{H3'\text{-}C3'\text{-}O\text{-}H}$ except in **1** where the torsion across C3′-O3′ bond is actually ε^- [C4′-C3′-O3′-P].

Karplus equation (2b), four dihedral [*i.e.* $\Phi_{H\text{-}C\text{-}O\text{-}H}$] solutions are possible for each of the $^3J_{H,OH}$ (Table 2 and Fig. 2): two in the cisoid domain (±30° to ±80°) and two in the transoid domain (±120° to ±150°). For **1**, the non-equivalent methylene protons (3b) of 3′-ethyphosphate moiety in DMSO-d_6 shows (<338 K) the presence of the intramolecular [2′-OH⋅⋅O3′] H-bonding promoting non-isochornacity, which collapses at a high temperature when H-bonding melts. The $^3J_{H2',OH}$ of 4.2 Hz and 6.1 Hz at 288 K for **1** and **3** respectively, characterize the unique solution of geometry optimized [with semi-empirical AM1 calculation as implemented in Gaussian 98 (4)] $\Phi_{H2',OH}$ in the positive transoid region, *i.e.* proximity towards O3′ (Fig. 2), thereby showing the presence of intramolecular 2′O-H⋅⋅O3′

Table 1. The Temperature Dependent Chemical Shift[a] (δ, in ppm) of 2′-, 3′- and 5′-OH for EtpA (**1**), 3′-dA (**2**), rA (**3**) and 2′-dA (**4**) in DMSO-d_6 at 500 MHz

TEMP (K)	Adenosine-3′-Ethylphosphate (EtpA)		3′-deoxy Adenosine (3′-dA)		Adenosine (rA)			2′-deoxy Adenosine (2′-dA)	
	$\delta_{2'OH}$	$\delta_{5'OH}$	$\delta_{2'OH}$	$\delta_{5'OH}$	$\delta_{2'OH}$	$\delta_{3'OH}$	$\delta_{5'OH}$	$\delta_{3'OH}$	$\delta_{5'OH}$
288	7.322	5.539	5.620	5.135	5.410	5.155	5.397	5.279	5.217
298	7.305	5.497	5.584	5.088	5.365	5.106	5.341	5.246	5.167
368	7.020	5.182	5.316	4.732	5.063	4.762	4.946	4.987	4.789

[a] Chemical shifts at the three representative temperatures (288 K, 298 K and 368 K) have only been shown.

Table 2. The Temperature Dependent $^3J_{HH}$ Coupling Constants Involving 2′-, 3′- and 5′-OH and Respective $\Phi_{H\text{-}C\text{-}O\text{-}H}$ Torsion Angle[a] for 50 mM/L for EtpA (**1**), 3′-dA (**2**), rA (**3**) and 2′-dA (**4**) in DMSO-d_6

TEMP (K)	Adenosine-3′-Ethylphosphate (EtpA)			3′-deoxy Adenosine (3′-dA)			Adenosine (rA)						2′-deoxy Adenosine (2′-dA)		
	$^3J_{H2'OH}$	Φ_1	$\Phi_{1'}$	$^3J_{H2'OH}$	Φ_1	$\Phi_{1'}$	$^3J_{H2'OH}$	Φ_1	$\Phi_{1'}$	$^3J_{H3'OH}$	Φ_2	$\Phi_{2'}$	$^3J_{H3'OH}$	Φ_2	$\Phi_{2'}$
288	4.2	± 45.9	± 123.5	4.3	± 45.2	± 124.0	6.1	± 34.0	± 133.2	4.5	± 44.0	± 125.1	3.8	± 48.7	± 121.4
298	4.1	± 46.5	± 123.0	4.3	± 45.2	± 124.0	6.1	± 34.0	± 133.2	4.5	± 44.0	± 125.1	3.4	± 51.0	± 119.3
368	0.8	± 71.2	± 100.3	3.6	± 49.6	± 120.3	1.0	± 70.0	± 102.4	0.4	± 76.8	± 94.8	0.2	± 81.7	± 90.0

[a] The torsion angles (Φ, in degree, see Figure 1) have been calculated using the Karplus equation $^3J_{HH} = 10.4\cos^2\Phi - 1.5\cos\Phi + 0.2^3$. Φ at the three representative temperatures (288 K, 298 K and 368 K) have only been shown.

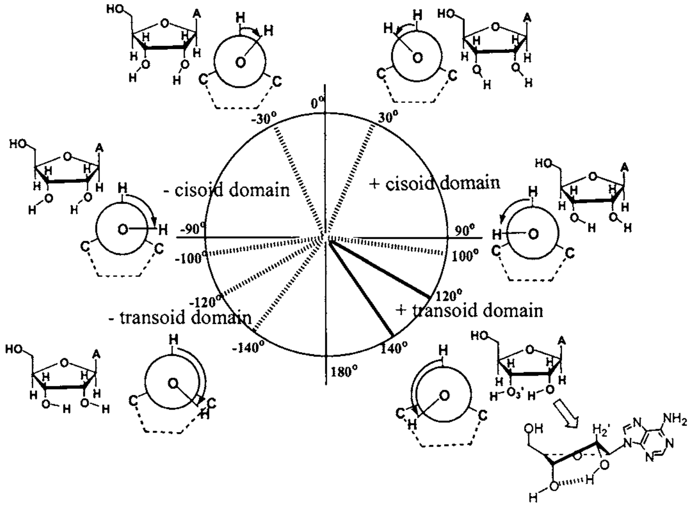

Figure 2. The torsional hyperspace for $\Phi_{\text{H-C-O-H}}$ as calculated from $^3J_{\text{H,OH}}$ (Table 2) using the Karplus equation $^3J_{\text{H,OH}} = 10.4 \cos^2 \Phi - 1.5 \cos \Phi + 0.2$ (2b) and also showing the relative proximity of the 2′- and 3′-OH at different torsional orientations. The $\Phi_{\text{H-C-O-H}}$ of the 2′-OH$_{\text{eq}}$ with S-type sugar conformation in positive transoid domain corresponds to the closest proximity to the neihbouring O3′.

H-bonding (ΔG°_{298K} : 1.8 kcal mol^{-1} for **1** and 2.0 kcal mol^{-1} for **3**). However, $^3J_{\text{H2}',\text{OH}}$ of 4.3 Hz for **2** and $^3J_{\text{H3}',\text{OH}}$ of 3.8 Hz for **4** indicate an extended minima of $-124.0^\circ \le \Phi_{\text{H2}',\text{OH}} \le 45.2^\circ$ for **2** and $-121.4^\circ \le \Phi_{\text{H3}',\text{OH}} \le 121.4^\circ$ for **4** at 288 K, thereby suggesting a flexible flip-flop nature of the solvated 2′-OH$_{\text{ax}}$ in **2** and 3′-OH$_{\text{ax}}$ in **4** due to the absence of any intramolecular interaction.

The less flexibility of the donor 2′-OH in the intramolecular H-bonding in **3** is due to the loss of conformational freedom compared to the acceptor 3′-OH, which is evident from their respective $-T\Delta S^\ddagger$: $[-T\Delta S^\ddagger]_{2'\text{-OH}} = -17.9$ kJ mol^{-1} and $[-T\Delta S^\ddagger]_{3'\text{-OH}} = -19.8$ kJ mol^{-1} at 298 K. The existence of weak long range $^4J_{\text{H2}',\text{OH3}'}$ in **3** (*i.e.* W conformation of H2′-C2′-C3′-O3′-H) indicates the

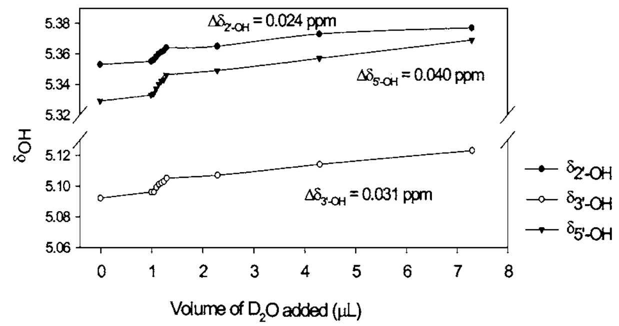

Figure 3. The plot of hydroxyl chemical shifts (δ_{OH}, in ppm) at 298 K as a function of volume of D_2O (in μL) added in the DMSO-d_6 solution of **3**.

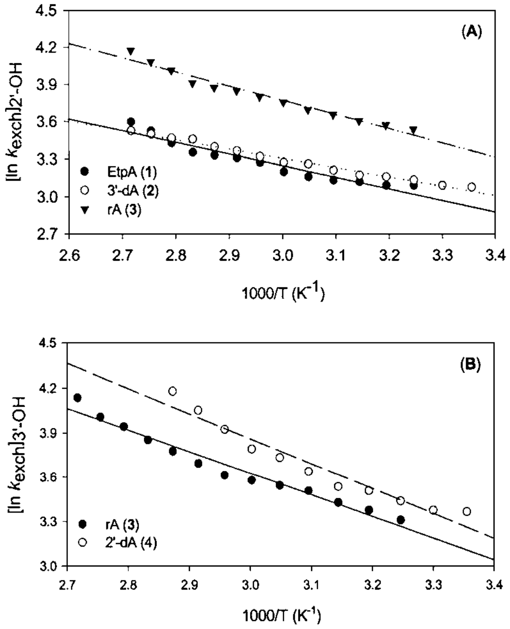

Figure 4. The activation enthalpy ($\Delta H^{\ddagger}$) and entropy ($\Delta S^{\ddagger}$) were calculated respectively from slope and intercept of the plot of $\ln k_{\text{exch}}$, measured from the lineshape analyses, as a function of inverse of the temperature and the free energy of activation $\Delta G^{\ddagger}$ at 298K ($\cong \Delta G^{\circ}_{298K}$ for H-bonding) by using the equation *viz.* $\Delta G^{\ddagger} = \Delta H^{\ddagger} - T\Delta S^{\ddagger}$ on the basis of reaction rate theory (2d,e). Panel (**A**) shows the plot of the $[\ln k_{\text{exch}}]_{2'\text{-OH}}$ for **1**, **2** and **3** as a function of the inverse of the temperature (1000/T, in K^{-1}) giving straight line with slope $= -0.93$ ($\sigma = \pm 0.08$), intercept $= 6.04$ ($\sigma = \pm 0.23$) and $R = 0.96$ for **1**; slope $= -0.73$ ($\sigma = \pm 0.03$), intercept $= 5.53$ ($\sigma = \pm 0.08$) and $R = 0.99$ for **2**; slope $= -1.15$ ($\sigma = \pm 0.06$), intercept $= 7.22$ ($\sigma = \pm 0.19$) and $R = 0.98$ for **3**. Panel (**B**) shows the plot of the $[\ln k_{\text{exch}}]_{3'\text{-OH}}$ for **3** and **4** as a function of the inverse of the temperature (1000/T, in K^{-1}) giving straight line with slope $= -1.46$ ($\sigma = \pm 0.08$), intervcept $= 8.01$ ($\sigma = \pm 0.24$) and $R = 0.98$ for **3**; slope $= -1.69$ ($\sigma = \pm 0.13$), intercept $= 8.92$ ($\sigma = \pm 0.42$) and $R = 0.97$ for **4**.

non-plausibility of the negative values in the cisoid and transoid domains (Fig. 2) among the all possible solutions of $\Phi_{H3',OH}$. So for $^{3}J_{H3',OH}$ of 4.5 Hz and $^{3}J_{H2',OH}$ of 6.1 Hz at 288 K in **3**, the NMR constrained torsional hyperspace scan shows the energy minima of the $\Phi_{H2',OH}$ involving 2′-OH$_{eq}$ at 133.2°, and for $\Phi_{H3',OH}$ involving 3′-OH$_{eq}$ at two distinct orientations of 44° and 125.1°, thereby showing H-bond-*accepting* 3′-OH is less restricted than that of H-bond-*donating* 2′-OH. The slow addition of D_2O in the DMSO-d_6 solution of **3** (50 mM/L) shows the relative change of δ_{OH} as $\Delta\delta_{2'\text{-OH}} = 0.024$ ppm $< \Delta\delta_{3'\text{-OH}} = 0.031$ ppm $< \Delta\delta_{5'\text{-OH}} = 0.040$ ppm (Fig. 3) which indicates the relative accessibility of water molecule at 2′- vis-a-vis 3′-OH compared to 5′-OH. Thus, in **3**, the poorer accessibility of water at 2′-OH show that it is the proton donor in the 2′-O-H$\cdots$O3′ intramolecular H-bonding. Besides, the ROESY spectra [Fig. 6] at 298 K for **3** in DMSO-d_6 shows a clear nOe contacts of water with both 2′ and 3′-OH. This suggesting the presence of the water bridge (2c) between the 2′/3′-OH and DMSO-d_6, supporting the energy minimized

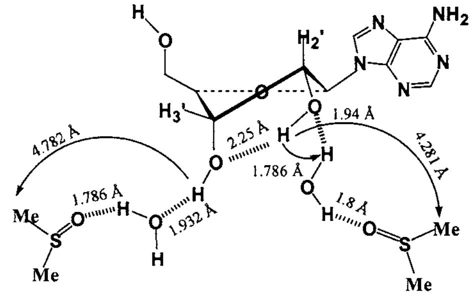

Figure 5. The mimicking model of the dynamic intra- as well as intermolecular H-bond in **3**, which in turn reflects the energetic preference for 2′-OH. Both the 2′- and 3′-OH in **3** are brigded with two molecules of water which are in turn intermolecularly attached to the DMSO-d_6. The energy minimization has been performed with SYBYL (v. 6.2) based on the Tripos Force Field with constraining endocyclic sugar torsion (from PSEUROT analyses (3)) along with $^3J_{H,OH}$ derived energy minimised $\Phi_{H2',OH}$, $\Phi_{H3',HO}$ (at 298 K) and keeping the $d_{2'OH...O3'}$ as 2.25 Å. The experimental ROESY contacts for both 2′- and 3′-OH to water also support the calculated inter-atomic distances between the hydroxyl group and the DMSO-d_6 for this energy minimized structure.

water solvated structure for **3** (Fig. 5) as perhaps the most viable model, although it is not the most energy minimized structure.

The NMR constrained conformational grid search for the energy minima of $d_{2'OH\cdots O3'}$ for **1** and **3** using SYBYL (v. 6.2), based on the Tripos Force Field and conjugate gradiant method, could however clearly indicate a long non-linear intramolecular H-bonded bridge and considerably smaller $\angle$O-H$\cdots$O3′ bond angle (1b) over the temperature range studied [2.2 Å(288 K) $\leq d_{2'OH\cdots O3'} \leq$ 2.75 Å(368 K) and 113.6° (288 K)$\leq \angle$O-H$\cdot\cdot$O3′ $\leq$ 93° (368 K)], thereby suggesting a relatively weaker 2′-OH$\cdots$O3′ H-bond in both of them. The ΔG°_{298K} for such weak non-linear

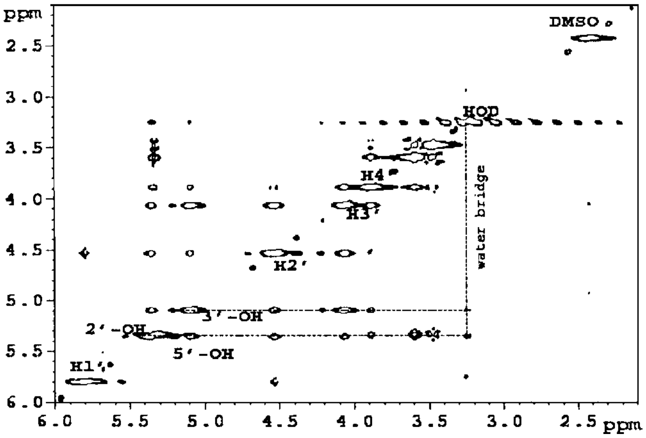

Figure 6. ROESY specturm of **3** (50 mM/L) in DMSO-d_6 at 298 K in 500 MHz. The cross peak of both 2′-OH and 3′-OH with HOD, present in DMSO-d_6, shows the proof of proposed water bridge.

H-bonding involving 2′- and 3′-OH in **1–4**, as calculated from the lineshape analyses of the hydroxyl resonances are close to the $\sim$2 kcal mol^{-1}.

ACKNOWLEDGMENTS

We thank the Swedish Board for Technical Development (TFR), the Swedish Natural Science Research Council (NFR), and the Swedish Board for Technical Development (NUTEK) for generous financial support. Thanks are due to the Wallenbergstiftelsen, ForskningsraÊ dsnämnden and the University of Uppsala for funds to purchase of 500-MHz and 600-MHz Bruker DRX NMR spectrometers.

REFERENCES

1. a) T. R. Cech, *Annu. Rev. Biochem.* **1990**, *59*, 543; b) G. A. Jeffrey, W. Saenger, *Hydrogen Bonding in Biological Systems*, Springer-Verlag, Berlin, **1991.**
2. a) G. A. Kumar, M. A. McAllister, *J. Org. Chem.* **1998**, *63*, 6968; b) R. R. Fraser, M. Kaufman, P. Morand, G. Govil, *Can. J. Chem.* **1969**, *47*, 403; c) P. H. Bolton, D. R. Kearns, *J. Am. Chem. Soc.* **1979**, *101*, 479; d) J. L Markley, W. M. Westler, *Biochemistry*, **1996**, *35*, 11092; e) J. Lin, P. A. Frey, *J. Am. Chem. Soc.* **2000**, *122*, 11258.
3. a) For review see: C. Thibaudeau, and J. Chattopadhyaya, *Stereoelectronic Effects in Nucleosides and Nucleotides and their Structural Implications*, (ISBN 91-506-1351-0), Department of Bioorganic Chemistry, Uppsala University Press (fax: +4618554495), Sweden, **1999** and references therein; b) J. Plavec, C. Thibaudeau, and G. Viswanadham, C. Sund, A. Sandström and J. Chattopadhyaya, *Tetrahedron* **1995**, *51*, 11775.
4. Gaussian 98 (Revision A.6), Gaussian, Inc., Pittsburgh PA, **1998**.

Downloaded At: 12:24 26 January 2011

Request Permission or Order Reprints Instantly!

Interested in copying and sharing this article? In most cases, U.S. Copyright Law requires that you get permission from the article's rightsholder before using copyrighted content.

All information and materials found in this article, including but not limited to text, trademarks, patents, logos, graphics and images (the "Materials"), are the copyrighted works and other forms of intellectual property of Marcel Dekker, Inc., or its licensors. All rights not expressly granted are reserved.

Get permission to lawfully reproduce and distribute the Materials or order reprints quickly and painlessly. Simply click on the "Request Permission/Reprints Here" link below and follow the instructions. Visit the U.S. Copyright Office for information on Fair Use limitations of U.S. copyright law. Please refer to The Association of American Publishers' (AAP) website for guidelines on Fair Use in the Classroom.

The Materials are for your personal use only and cannot be reformatted, reposted, resold or distributed by electronic means or otherwise without permission from Marcel Dekker, Inc. Marcel Dekker, Inc. grants you the limited right to display the Materials only on your personal computer or personal wireless device, and to copy and download single copies of such Materials provided that any copyright, trademark or other notice appearing on such Materials is also retained by, displayed, copied or downloaded as part of the Materials and is not removed or obscured, and provided you do not edit, modify, alter or enhance the Materials. Please refer to our Website User Agreement for more details.

Order now!

Reprints of this article can also be ordered at
http://www.dekker.com/servlet/product/DOI/101081NCN100002521